




## Article

# Stochastic Wind Power Generation Planning in Liberalised Electricity Markets within a Heterogeneous Landscape

Lennard Sund <sup>1,\*</sup> , Saber Talari <sup>1,\*</sup>  and Wolfgang Ketter <sup>1,2,\*</sup> <sup>1</sup> Faculty of Management, Economics and Social Sciences, University of Cologne, 50923 Cologne, Germany<sup>2</sup> Rotterdam School of Management, Erasmus University Rotterdam, 3062 PA Rotterdam, The Netherlands

\* Correspondence: talari@wiso.uni-koeln.de (S.T.); ketter@wiso.uni-koeln.de (W.K.)

**Abstract:** Spatially separated locations may differ greatly with respect to their electricity demand, available space, and local weather conditions. Thus, the regions that are best suited to operating wind turbines are often not those where electricity is demanded the most. Optimally, renewable generation facilities are constructed where the maximum generation can be expected. With transmission lines limited in capacity though, it might be economically rational to install renewable power sources in geographically less favourable locations. In this paper, a stochastic bilevel optimisation is developed as a mixed-integer linear programme to find the socially optimal investment decisions for generation expansion in a multi-node system with transmission constraints under an emissions reduction policy. The geographic heterogeneity is captured by using differently skewed distributions as a basis for scenario generation for wind speeds as well as different opportunities to install generation facilities at each node. The results reinforce that binding transmission constraints can greatly decrease total economic and emissions efficiency, implying additional incentives to enhance transmission capacity between the optimal supplier locations and large demand centres.

**Keywords:** renewable expansion planning; emission policy; transmission constraints; constrained optimisation; stochastic optimisation; bilevel programming



**Citation:** Sund, L.; Talari, S.; Ketter, W. Stochastic Wind Power Generation Planning in Liberalised Electricity Markets within a Heterogeneous Landscape. *Energies* **2022**, *15*, 8109. <https://doi.org/10.3390/en15218109>

Academic Editor: Abu-Siada Ahmed

Received: 30 September 2022

Accepted: 24 October 2022

Published: 31 October 2022

**Publisher's Note:** MDPI stays neutral with regard to jurisdictional claims in published maps and institutional affiliations.



**Copyright:** © 2022 by the authors. Licensee MDPI, Basel, Switzerland. This article is an open access article distributed under the terms and conditions of the Creative Commons Attribution (CC BY) license (<https://creativecommons.org/licenses/by/4.0/>).

## 1. Introduction

### 1.1. Motivation

Electricity generation constitutes a considerable driver of total greenhouse gas (GHG) emissions. Between 2012 (27.4%) and 2019 (26.5%), its share in global carbon dioxide (CO<sub>2</sub>) emissions remained relatively unchanged while total emissions from electricity generation even increased by about 2% [1]. The power sector's relevance with respect to decarbonisation is much stronger still in some regions. In Africa and Asia-Oceania in 2019, carbon emissions from electricity generation accounted for 37.3% and 41.9% of each region's emissions, respectively. Thus, with global GHG emissions remaining at levels far beyond their climatically sustainable degree [2], it is evident that the decarbonisation of the power sector is one of the most pressing issues of today's energy policy.

The electrification of processes which have previously been fuelled by fossil energy carriers, such as mobility and certain industrial operations, will put additional stress on power systems. This makes quickly ramping up renewable energy sources (RES) all the more important. However, making the switch to an RES-dominated power sector entails strategical and operational challenges. The central difficulty in dealing with wind- and solar power, which are likely to overtake hydro as the most prevalent RES [3], is that the decision when and where to produce electricity is beyond the control of the RES operators. These sources fully depend on uncertain weather conditions. Even more so, weather conditions are geographically heterogeneous. This means that the ideal sites for generation units are often not located where the relevant load accrues, placing additional burdens on transmission grids.

Additionally, wind- and solar power, while coming at practically zero marginal cost and with several other benefits (for an overview, see [4] p. 20 et seq.), in the short run, greatly increase the system cost of power generation when compared to fossil fuels due to their initial investment cost. Moreover, while the causal relationship between energy usage and economic growth is still surprisingly unclear, energy usage per capita is highly positively correlated with per capita GDP [5]. Thus, political entities nowadays face the difficult trade-off between (short-term) economic performance and reducing GHG emissions. In order to support this demanding decision-making process, we aim to answer the following research question:

**Research Question:** Taking generation stochasticity and optimal operational decisions in a geographically heterogeneous landscape into account, how can policy-makers make optimal decisions about the trade-off between system cost and GHG emissions with respect to their preferences?

To inform deciders on questions revolving around multiple goals, multi-objective optimisations are a frequently used approach (for an overview of used techniques of multi-objective optimisations in the context of energy systems, see [6]). To more accurately handle the uncertainty associated with the generation of renewable energy sources and the consequent operational decisions, we develop a multi-objective bilevel stochastic mathematical programme. Our results emphasise the efficiency gains in combined planning efforts of environmental and economic goals and the importance of sufficient transmission capacity. Moreover, they imply that, even at elevated factor prices, natural gas is likely to stay relevant in electricity generation, particularly with a stricter GHG emissions regime.

## 1.2. Related Literature

Our work is situated within the broader field of energy systems planning and operation optimisation. In particular, it belongs to the research on generation (and transmission) expansion planning (G&TEP) and is closely related to three streams in this field.

It firstly relates to the multi-objective optimisation literature. Energy systems optimisation has increasingly applied multi-objective functions to explicitly model the associated trade-offs. Traditionally, the problem was regarded either from the perspective of a social planner who wants to minimise costs or from the perspective of a market actor who wants to maximise profits (for an overview, see [7]). This cost-based view has been complemented with other objectives. The most prevalent additions are the control of emissions of noxae like CO<sub>2</sub> or CH<sub>4</sub> [8–10] and the reliability of the power supply [11–13]. Within multi-objective optimisation literature concerned with the emissions of noxae, different problem setup- and solution techniques are used. A relatively new approach is using bilevel models with one objective on the first level and the other on the second to find optimal outcomes. These models are solved using methods such as joint probabilistic programming and fuzzy optimisation [14] or convergent mathematical optimisation (after applying a decomposition like [15]). Another approach to solving multi-objective problems is searching for non-dominated solutions, that is, those that are not strictly mathematically inferior to other solutions. The identified points lie on the so-called Pareto-frontier. Since there are typically infinitely many Pareto-optimal solutions [16], evolutionary algorithms are often employed to find a representative set [17]. Commonly used techniques are particle swarm optimisation and the non-dominated sorting genetic algorithm II (NSGAI) [6]. The advantage of this approach is that no preference- and size relations have to be known a priori. On the downside, the optimisation is non-convergent. If one wishes to obtain converging solutions, the multi-objective problem has to be reformulated as a single-level function to then solve it using mathematical optimisation. The common methods to transform the optimisation problem this way are weighted sum [16],  $\epsilon$ -constraint [18], goal attainment [19] and goal programming [20]. The disadvantages using this approach are that it is computationally quite taxing to find the Pareto-frontier and that profound knowledge of the relation of both objectives is required to make them comparable in a single equation [6].

Furthermore, we draw on the literature of stochastic optimisation in power systems. Deterministic models in G&TEP assume that the expansion planner has perfect foresight and are thus able to greatly reduce the computational burden associated with solving them. This disregard for the manifold uncertainties in energy markets constitutes an oversimplification though that could induce far from optimal decisions [21]. In reality, uncertain weather conditions lead to stochastic RES generation [22–24], future prices are unforeseeable [25], the behaviour of market competitors is unknown [26], and generation costs, demand fluctuations and demand growth are uncertain [23,24]. Moreover, actors often can neither control future network performance nor regulatory risk [17]. Some researchers address this uncertainty with either scenario analyses [27] or sensitivity analyses [17]. The most commonly used method in stochastic optimisation, though, is stochastic programming, in which scenario generation (like Monte Carlo simulation) and scenario reduction (using clustering algorithms) are employed to discretise probability density functions into scenarios with respective probabilities [9,23,24,28,29].

In addition, our research relates to the literature on bilevel optimisation. Bilevel optimisation is used to solve the actions of players in hierarchical games. Those consist of one or more leaders who take their turn first, as well as one or more followers who perform their action(s) after observing the leader's actions. The leader(s) moreover anticipate the followers' reaction(s) to their own decision(s). One example of these sequential games are the well-known Stackelberg games [30]. In energy systems optimisation, this is used to model competitive markets and auctions [31,32], the interplay between transmission system operators and generation companies [29], and the relations between upper- and lower level political entities [14].

Another application in the context of G&TEP problems is using the upper level to decide on optimal investment, while using the lower level to explicitly model optimal market clearing dependent on the upper level decisions from a pure social welfare perspective. Using this approach in a stochastic bilevel optimisation, this can lead to quite taxing computations, since a multitude of scenarios has to be considered on both levels. Opting for explicitly modelling market clearing in a bilevel stochastic G&TEP problem results in a more exact technical representation of generation and transmission operations in each considered scenario. Valle et al. [11], for instance, have modelled a gas infrastructure investment with explicit market clearing and [33] used this approach for an energy storage system planning problem. On the other hand, this usually entails choosing a limited number of nodes, generation technologies, and scenarios to avoid encountering computational infeasibility. Many studies regarding policy in G&TEP problems opt for not explicitly optimising market clearing due to this reason [14,15,23,34].

Table 1 shows the literature most closely related to our work and how it fits into it. As can be seen, the G&TEP literature is thus far mostly concerned with the policy level on a larger scale on the one hand, in which a deterministic bilevel optimisation is used to determine optimal levels of investment and operation under perfect foresight. This is sometimes combined with a multi-objective approach to account for distinct policy goals. While being more easily scalable, this only insufficiently addresses the stochastic nature of RES that are essential to decarbonising the power system. When making policy decisions for a smaller area, one can expect more efficient decisions on policy and investment plans when the stochasticity of e.g., wind speeds is also taken into account.

On the other hand, the part of the G&TEP literature that is concerned with the uncertainty of RES usually does not deal with explicit operational decisions, and, if so, seldom taking a policy perspective, particularly not under consideration of the social detriment of GHG emissions. Thus far, the only studies considering emissions and system cost in stochastic bilevel models are [14,15]. Still, these authors also do not use the lower level to model optimal market clearing, but rather to coordinate between different policy levels. Therefore, to the best of our knowledge, there is not yet a study analysing the optimal decisions of a social planner conjointly considering both emissions and expected generation cost, taking the relevant uncertainty of RES into account. By making this decision conjointly,

with the operational realities of realistic scenarios in mind, one could achieve substantial gains in efficiency.

**Table 1.** Classification of the closest related literature

Source	Multiobjective	Stochastic	Bilevel
[9]	Emissions, Cost, Revenue	RES Generation	
[13]	Emissions, Cost, Reliability	Peak Load Surplus	
[22]	Infrastructure Cost, Operation Cost, Emissions	Wind	
[12]	Cost, Voltage Stability	Load, Wind	
[8]	Emissions, GDP, Energy Consumption		National/Regional Level
[11]	Demand Utility, Cost		Investment, Operation
[33]	Cost load Shaving, Volatility, Reserve Capability		Investment, Operation
[34]			Investment, Operation
[18]		Wind	Area-Coordination
[29]		Wind	
[27]		Multiple	
[23]		Load, Wind	
[24]		Load, Wind	
[28]		Load, Wind	
[10]	Emissions, Cost, Generation		
[14]	Emissions, Cost	Load	Emissions-Cost-trade-off
[15]	Emissions, Cost	Load	Cost-Emissions-trade-off
This Study	Emissions, Cost	Wind	Investment, Operation

On a broader level, our research is related to the literature on renewable energy sources and how they can be employed to reach GHG neutrality. Researchers from the economics profession have put a focus on innovation and how a policy mix of hard emission reduction policy and innovation subsidies can foster the transition to a carbon-neutral economy [35,36]. Researchers from the field of social- and environmental studies moreover emphasise the need for a concerted global policy action, including considerable GHG emission prices on all sources, major subsidies to innovation in more efficient use, generation, and mitigation technologies, investment in natural sinks as well as GHG-neutral or net negative infrastructure construction as well as an overhaul of the electricity market design [37,38]. Besides investment, innovation, and regulation, it is also important to take public sentiment into account. Reviewing literature on renewable energies, Qazi et al. [39], for instance, find that public reservations against the installation are often a hindrance in the rollout of RES.

### 1.3. Contribution and Organisation

We aim to fill the gap in research elaborated in Section 1.2 by developing a multi-objective GEP-model that uses its bilevel structure to explicitly analyse the optimal operational decisions under a high degree of uncertainty of wind power generation under heterogeneous weather conditions. Therein, we take the perspective of a social planner in charge of the introduction an emission reduction policy and the development of an investment plan. Our approach allows decision-making based on the conjoint optimisation of system cost and GHG emissions, informed by more realistic situational operation decisions and constraints. We differ from the existing literature as we decide to focus on the decision level of a smaller scale political entity to be able to incorporate more realistic operational responses to uncertain wind power realisations.

By properly accounting for market clearing in each considered scenario, our model can point out optimal generation expansions given any particular a priori preference relation between costs and emissions. When compared to other research dealing with similar issues, we contribute to the literature by simultaneously:

- developing a stochastic bilevel optimisation model for a multi-nodal GEP problem, taking into account the heterogeneity in the suitability for the generation of renewable energy of different locations;
- conjointly optimising the policy decision on the introduction of an emissions-reduction regulation and the investment decisions into different generation assets to increase societal efficiency;
- explicitly accounting for operational decisions in a heterogeneous stochastic landscape with a (potentially) high penetration of RES;
- recasting the multi-objective problem into a single objective to be able to find convergent optima instead of using heuristic search, given the social planner's preferences on GHG emissions;
- applying our model to a realistic use case, relying on real world data combined with a Monte Carlo scenario generation and -reduction approach to draw conclusions on its implications for the real world.

The rest of this paper is structured as follows: In Section 2, we develop our bilevel stochastic programme and discuss our solution strategy. We elaborate the setup for the experiment we test our model on as well its results in Section 3. We then discuss our findings in Section 4 and conclude in Section 5.

## 2. Methods

In this section, we develop a static stochastic programme to solve the multi-objective GEP problem. To this end, we thoroughly discuss our approach in Section 2.1. We then present the mathematical problem formulation in Section 2.2 and elaborate our strategy to solving the bilevel formulation in Section 2.3.

### 2.1. Problem Statement

We optimise both the strategical long-term planning decision as well as short-term operational decisions in every possible considered situation in a GEP-model. On the one hand, we consider the perspective of a social planner who has to trade off the total cost of generation and expansion against the social detriment associated with GHG emissions. This social planner is in charge of simultaneously deciding upon investing in new generation facilities and a policy limiting the annual emissions of GHG. At the same time, she will take the ramifications that her decisions have on possible operational choices into account. We moreover optimise the operational decisions in every considered stochastic wind power scenario by minimising total operational cost. The total system cost is then given by investments in candidate generation units as well as total variable cost of generation.

Here, a static case is considered. This means that the investment decisions made “here-and-now” have to suffice for all situations which may be encountered, when “wait-and-see” dispatch decisions have to be made, since there is no additional opportunity within the planning horizon to adjust the decisions made at the first stage. We moreover consider a long-term planning horizon (for instance, the lifespan of a wind turbine is taken to be approximately 25 years [40]). Furthermore, we analyse an operational period of one year, using annualised cost of investment and maintenance, as is a standard procedure (see, e.g., [7]). Thus, the objective function is expressed in annualised cost as well.

As an example, we assume that the territorial unit that the social planner is in charge of has an installed base of coal power plants and that she can consider investing in wind-and/or natural gas turbines. Because of the international commitment towards limiting global warming, we do not allow for constructing additional coal power plants in our specification. However, this could easily be added.

In order to tackle this problem structure, a bi-level approach is taken. Each level represents the different stage of decision-making, as well as different costs accruing. On the upper level, the amount of investment in each asset at each node is decided upon, taking into account the cost ensuing at the generation phase, depending on these investment



decisions. Moreover, the social planner decides on an emissions' reduction policy, taking into account the GHG emissions accruing at the dispatch level.

On the lower level, we also take a social planner perspective, in the sense that it is the objective of the lower level optimisation to minimise the total operational cost in every single scenario and load demand level, given the decisions made on the upper level. As opposed to the upper level decision-making, here, GHG emissions from generation are not considered, but total emissions are constrained by the upper level policy decision. More precisely, given each realisation of wind power at every node and the level of load demand, the social planner decides upon dispatching electricity generated through wind- or natural gas turbines or coal power plants. She can also choose not to dispatch the entirety of the demanded electricity, thereby suffering a considerable loss of load penalty. Since part of our target is finding an optimal emissions' policy, given the policymakers valuation of the societal detriments of GHG emissions, they do not enter the lower level's objective function. Instead, overall emissions are constrained by a general policy parameter decided upon on the upper level. A schematic overview over the proposed model structure is shown in Figure 1.

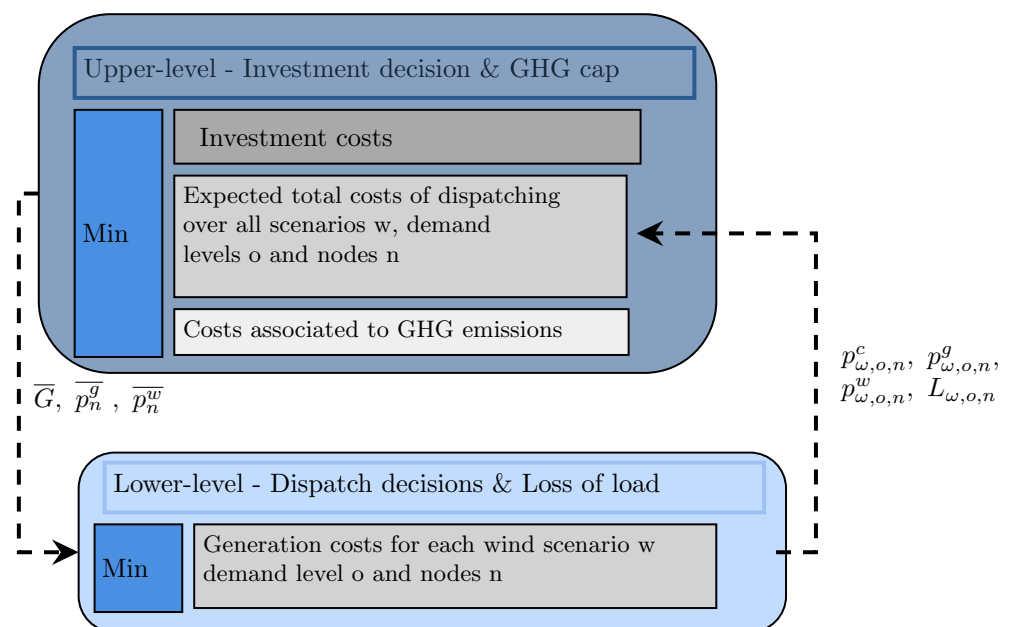


**Figure 1.** Schematic overview of the proposed model structure.

Moreover, the territorial unit in question is assumed to have a heterogeneous landscape. Therefore, the weather conditions governing renewable electricity generation are also much different between the distinct locations. In our example, we consider a multi-node system with diverse characteristics of weather conditions, load demand, and spatial capacity in each location as is described in Section 3.1.

Additionally, the power flow between nodes is restricted by the capacity of the installed transmission lines. This is particularly relevant in the examined case with heterogeneous weather conditions. Since some areas are better suited than others for renewable energy production, a limited transmission capacity could severely hinder the efficient adoption of zero emission energy sources throughout the policy area. We also assume that wind power generation can be curtailed at any time without any cost or reimbursement.

## 2.2. Problem Formulation

### 2.2.1. Multi-Objective Formulation

On the upper level of the analysed problem setup, the social planner is considering two objectives—total cost and total GHG emissions. This presents a challenge, since both objectives are difficult to compare and measured in different units of account. Below, we explicate the used representation of both and how we implement the trade-off. The total system cost is given by the overall cost of investment in additional generation capacity as well as the expected cost of operation, as shown in (1):

$$\sum_{n=1}^N (I^w \overline{p}_n^w + I^g \overline{p}_n^g) + \sum_{o=1}^O \rho_o \sum_{\omega=1}^{\Omega} \Phi_{\omega} \sum_{n=1}^N (c^c p_{\omega,o,n}^c + c^g p_{\omega,o,n}^g + c^L L_{\omega,o,n}) \quad (1)$$

The term on the left-hand-side of (1) represents the expected total investment cost over all assets at all nodes  $n$ . Variables  $\overline{p}_n^w$  and  $\overline{p}_n^g$  denote the additional capacity installation at each node for wind- and gas turbines, respectively, while  $I^w$  and  $I^g$  denote their respective annualised investment cost per MW installed. The right-hand-sided term of (1) is the expected total cost of dispatching over all demand levels  $o$ , all scenarios  $\omega$ , and all nodes  $n$ . The parameters  $\rho_o$  and  $\Phi_{\omega}$  are the hours per year in operating condition  $o$ , and the probability of wind power scenarios  $\omega$ , respectively. The amount of power supplied by coal (gas) and their respective unit costs are denoted by  $p_{\omega,o,n}^c$  ( $p_{\omega,o,n}^g$ ) and  $c^c$  ( $c^g$ ).  $L_{\omega,o,n}$  is the loss of load, i.e., the amount of demanded load that can't be supplied, and  $c^L$  is the associated cost incurred per unit of lost load. Wind power dispatch does not enter the objective function, since it has a marginal production cost of zero.

Besides the total system cost, the social planner is also concerned with lowering GHG emissions. These are determined by multiplying the expected amount of MWh produced by each means of generation with their associated per unit emissions. In the considered scenario, total emissions are thus given by:

$$\sum_{o=1}^O \rho_o \sum_{\omega=1}^{\Omega} \Phi_{\omega} \sum_{n=1}^N [p_{\omega,o,n}^c G^c + p_{\omega,o,n}^g G^g], \quad (2)$$

where  $G^c$  and  $G^g$  are the amount of CO<sub>2</sub>-equivalent (CO<sub>2</sub>eq) GHG emissions associated with one MWh of electrical energy generated by use of coal power plants and gas turbines, respectively. The social planner now faces the problem of comparing and weighting these two targets. There are multiple ways to do this. We explain our approach in more detail below.

In multi-objective optimisation problems, we deal with two or more objectives that are frequently not denoted in the same unit. There is a multitude of solution approaches used to solve these type of problems as elaborated in Section 1.2. The most frequently used ones are Particle Swarm Optimisation and NSGAII [6]. We opt for recasting the multi-objective optimisation problem as a single-objective function using the weighted sum method, though, with the social cost of carbon as the weighting parameter. Using the weighted sum method, one expresses all considered objective functions of a multi-objective problem in a single objective function, which can then be solved in the same manner as a single-objective optimisation. This is achieved by adding both objectives and multiplying each with a weighting parameter (see, e.g., [16]). Often, parameters are chosen so that they add up to one, mostly for clarity. Instead, we opt for expressing the expected damages from emissions in monetary terms.

We do so because, even though not exact, the social cost of GHG emissions is a relatively well established research field which enables a sensible operationalisation (for a review, see [41]). At the same time, this allows us to solve the problem using mathematical optimisation, thus ensuring finding global optima given a respective preference relation (Other commonly used techniques like genetic algorithms arrive at approximately optimal solutions, as they are non-convergent heuristic methods). We therefore consider SCC as

a function that maps the total emitted amount of CO<sub>2</sub>eq GHG to their societal detriment. While possible atmospheric tipping points are of concern, we follow a large part of the environmental economics literature and take SCC to be a linear function of (2) (see [35,36]). In other words, SCC can be considered as the constant-value societal cost per unit of CO<sub>2</sub>eq emissions. We moreover do not assume any particular value for SCC. While there are some boundaries on realistic values provided by the literature (e.g., [41]), this is ultimately a value judgement dependent on the policymakers preferences. Therefore, the upper level objective function is given by:

$$\begin{aligned} \min_{\Delta_{UL}} \quad & \sum_{n=1}^N (I^w \overline{p}_n^w + I^g \overline{p}_n^g) + \sum_{o=1}^O \rho_o \sum_{\omega=1}^{\Omega} \Phi_{\omega} \sum_{n=1}^N (c^c p_{\omega,o,n}^c + c^g p_{\omega,o,n}^g + c^L L_{\omega,o,n}) \\ & + SCC \cdot \sum_{\omega=1}^{\Omega} \Phi_{\omega} \sum_{o=1}^O \rho_o \sum_{n=1}^N (p_{\omega,o,n}^c G^c + p_{\omega,o,n}^g G^g), \end{aligned} \quad (3)$$

where  $\Delta_{UL}$  are the upper level decision variables, and SCC is the linear social cost of carbon per unit of CO<sub>2</sub>eq emission.

### 2.2.2. Bilevel Formulation

The optimisation of the upper level objective elaborated in Section 2.2.1 is constrained by:

$$s.t. \left\{ \begin{array}{l} \overline{p}_n^w = \sum_q u_{nqa}^{opt} P_{nqa=w}^{opt} \end{array} \right. \quad (4)$$

$$\overline{p}_n^g = \sum_q u_{nqa}^{opt} P_{nqa=g}^{opt} \quad (5)$$

$$\sum_q u_{nqa}^{opt} = 1 \quad (6)$$

$$u_{nqa}^{opt} \in \{0, 1\} \quad \forall q \quad \left. \vphantom{u_{nqa}^{opt}} \right\} \forall n, a \quad (7)$$

$$\overline{G} \geq 0 \quad (8)$$

$$p_{\omega,o,n}^c, p_{\omega,o,n}^g, L_{\omega,o,n} \in \Theta_{\omega,o,n}(d_{o,n}, W_{\omega,n}, \overline{p}_n^w, \overline{p}_n^g, \overline{G}) \quad \forall \omega, o, n. \quad (9)$$

Constraints (4)–(7) regard the investment decisions. Investments can only be made between multiples of  $P_{nqa}^{opt}$ , where  $a$  denotes the asset class, and  $q$  the size of the investment decision. Equation (6) enforces that, for each asset at each node, there is exactly one investment decision (including the option not to invest at all) and (7) makes decision variable  $u_{nqa}^{opt}$  binary.  $\overline{G}$  is the GHG-cap, i.e., the maximum cumulative amount of CO<sub>2</sub>eq GHG emissions over all nodes and every load demand level  $d_o$ , and is enforced to be non-negative in (8). Finally, (9) states that the generation of each generating unit in each case at each node as well as the amount of load demand not serviced is determined by a separate market clearing optimisation  $\Theta_{\omega,o,n}$  (the lower level problem).  $\Delta_{UL} = \{\overline{p}_n^w, \overline{p}_n^g, \overline{G}, u_{nqa}^{opt}\}$  are the upper level decision variables. The optimal values for the lower level's decision variables,  $p_{\omega,o,n}^c$ ,  $p_{\omega,o,n}^g$ , and  $L_{\omega,o,n}$ , in turn, depend on the upper level decisions, maximum generation capacities of the candidate generation units  $\overline{p}_n^w$  and  $\overline{p}_n^g$ , the decision on the emissions cap  $\overline{G}$ , as well as the realised combination of wind power in each scenario  $W_{\omega,n}$  and the load demand levels  $d_o$ .

On the lower level, the overall emissions are constrained by GHG-cap  $\overline{G}$  that was decided upon on the upper level. The lower level problem coordinating optimal market clearing throughout all weather scenarios and load levels in a year is thus given by:



$$\Theta_{\omega,o,n} (d_{o,n}, W_{\omega,n}, \bar{p}_n^w, \bar{p}_n^c, \bar{G}) = \quad (10)$$

$$\left\{ \begin{array}{l} \text{Min.} \sum_{n=1}^N [c^c p_{\omega,o,n}^c + c^g p_{\omega,o,n}^g + c^L L_{\omega,o,n}] \end{array} \right. \quad (11)$$

$$\text{s.t. } p_{\omega,o,n}^w + p_{\omega,o,n}^c + p_{\omega,o,n}^g + L_{\omega,o,n} - f_{\omega,o,n}^f + f_{\omega,o,n}^t = d_{o,n} : \lambda_{\omega,o,n} \quad \forall n \quad (12)$$

$$0 \leq p_{\omega,o,n}^w \leq \bar{p}_n^w W_{\omega,n} : \mu_{\omega,o,n}^w \quad \forall n \quad (13)$$

$$0 \leq p_{\omega,o,n}^c \leq \bar{p}_n^c : \mu_{\omega,o,n}^c \quad \forall n \quad (14)$$

$$0 \leq p_{\omega,o,n}^g \leq \bar{p}_n^g : \mu_{\omega,o,n}^g \quad \forall n \quad (15)$$

$$0 \leq L_{\omega,o,n} \quad \forall n \quad \left. \vphantom{\sum_{n=1}^N} \right\} \forall o, \omega \quad (16)$$

$$\sum_{n=1}^N \sum_{o=1}^O \rho_o [p_{\omega,o,n}^c G^c + p_{\omega,o,n}^g G^g] \leq \bar{G} : \alpha_{\omega} \quad \forall \omega. \quad (17)$$

Here,  $\Delta_{LL} = \{p_{\omega,o,n}^w, p_{\omega,o,n}^c, p_{\omega,o,n}^g, f_{\omega,o,n}^f, f_{\omega,o,n}^t, L_{\omega,o,n}\}$  are the lower level decision variables. Equation (11) is the lower level objective and minimises generation cost for every wind condition  $W_{\omega,n}$  at all times for all nodes. Equation (12) ensures that the electricity market is always cleared. Specifically, it enforces that the cumulative generation of all assets at any given node plus its power flow balance and its loss of load always equal the local power demand. Variables  $f_{\omega,o,n}^f$  and  $f_{\omega,o,n}^t$  denote the power flowing through the transmission line “from” and “to” node  $n$ , respectively. Therefore, a property of any node  $n$  is a collection of one or more lines leading “to” and “away from” it. Note that the power flow can be negative though. Thus, “from” and “to” are rather a measure of accounting than directional information. Constraints (13)–(15) ensure non-negativity of power generation and that neither asset produces more than its capacity. In (13), the term  $W_{\omega,n}$  describes the wind power generated at node  $n$  in scenario  $\omega$  and determines at which proportion of the installed capacity the wind turbines can operate. Variables  $\lambda_{\omega,o,n}$ ,  $\mu_{\omega,o,n}^w$ ,  $\mu_{\omega,o,n}^c$ ,  $\mu_{\omega,o,n}^g$  are the dual variables of (12)–(15). The dual variable of the market clearing Equation (12),  $\lambda_{\omega,o,n}$ , can be interpreted as the marginal nodal price of generation, i.e., the marginal value created through an additional unit of power received at node  $n$ . The others can be interpreted as the shadow prices of each production asset. In other words, they represent the improvement of social welfare ensuing from a marginal increase in the respective production facility. Equation (16) ensures that the loss of load is always non-negative. Finally, (17) represents the emissions’ reduction policy. More specifically, it restricts the overall amount of CO<sub>2</sub>eq GHG emissions in a year to  $\bar{G}$ , the GHG-cap decided upon in the upper level. The dual variable of (17) is denoted  $\alpha_{\omega}$ .

The transmission constraints are specified below:

$$\left\{ \begin{array}{l} -\bar{f}_l \leq f_{o,\omega,l} \leq \bar{f}_l : \mu_{o,\omega,l}^{\bar{f}}, \mu_{o,\omega,l}^{\underline{f}} \quad \forall l \end{array} \right. \quad (18)$$

$$f_{o,\omega,l} = S_l (\delta_{o,\omega,l}^f - \delta_{o,\omega,l}^t) : \mu_{o,\omega,l}^f \quad \forall l \quad (19)$$

$$-\pi \leq \delta_{o,\omega,n} \leq \pi : \mu_{o,\omega,n}^{\bar{\delta}}, \mu_{o,\omega,n}^{\underline{\delta}} \quad \forall n \quad (20)$$

$$\left. \begin{array}{l} \delta_{o,\omega,1} = 0 : \mu_{o,\omega,1}^{\delta_{ref}} \end{array} \right\} \forall o, \omega \quad (21)$$

Equation (18) reads that any power flow  $f_{o,\omega,l}$  through line  $l$  cannot ever exceed its line capacity  $f_l$ . Note again that every line  $l$  leads “from” a node “to” another node. The power flow is governed by the voltage angle between the sending and the receiving node,  $\delta_{o,\omega,l}^f$  and  $\delta_{o,\omega,l}^t$ , respectively, as specified by (19). Parameter  $S_l$  denotes the susceptance of line  $l$ . The maximum voltage angle at any node  $n$  is confined to  $\pm \pi$  in (20). Ultimately, (21) sets the voltage angle at reference node  $n = 1$  to zero. Terms  $\mu_{o,\omega,l}^{\bar{f}}, \mu_{o,\omega,l}^f, \mu_{o,\omega,l}^{\bar{t}}, \mu_{o,\omega,n}^{\bar{\delta}}, \mu_{o,\omega,n}^{\delta}$ , and  $\mu_{o,\omega,1}^{\delta_{ref}}$  denote the respective dual variables.

### 2.3. Solution Strategy

We solve the problem by transforming it to a single-level mixed-integer problem. Bilevel problems can be solved by transforming the lower level problem in its respective dual problem [42]. The lower level constraints given in (10)–(21) are all convex and continuous, which, implying that strong duality holds [43], i.e., that the optimal values of the dual problem equal those of the primal problem. Below, (22)–(30) define the dual problem formulation of the market clearing problem:

$$\left\{ \begin{array}{l} \sum_{n=1}^N c^c p_{\omega,o,n}^c + \sum_{n=1}^N c^g p_{\omega,o,n}^g + \sum_{n=1}^N c^L L_{\omega,o,n} = \\ \sum_{n=1}^N \lambda_{\omega,o,n} d_{o,n} - \sum_{n=1}^N \mu_{\omega,o,n}^{\bar{w}} \bar{p}_n^{\bar{w}} \cdot W_{\omega,n} - \sum_{n=1}^N \mu_{\omega,o,n}^{\bar{c}} \bar{p}_n^{\bar{c}} - \sum_{n=1}^N \mu_{\omega,o,n}^{\bar{g}} \bar{p}_n^{\bar{g}} \end{array} \right. \quad (22)$$

$$-\lambda_{\omega,o,n} + \mu_{\omega,o,n}^{\bar{w}} \geq 0 \quad \forall n \quad (23)$$

$$c^c - \lambda_{\omega,o,n} + \alpha_{\omega} \cdot \rho_o G^c + \mu_{\omega,o,n}^{\bar{c}} \geq 0 \quad \forall n \quad (24)$$

$$c^g - \lambda_{\omega,o,n} + \alpha_{\omega} \cdot \rho_o G^g + \mu_{\omega,o,n}^{\bar{g}} \geq 0 \quad \forall n \quad (25)$$

$$c^L - \lambda_{\omega,o,n} \geq 0 \quad \forall n \quad (26)$$

$$\lambda_{o,\omega,l}^f - \lambda_{o,\omega,l}^t - \mu_{o,\omega,l}^f + \mu_{o,\omega,l}^{\bar{f}} - \mu_{o,\omega,l}^{\bar{t}} = 0 \quad \forall l \quad (27)$$

$$\sum_{n^f} S_l \mu_{o,\omega,l}^f - \sum_{n^t} S_l \mu_{o,\omega,l}^{\bar{f}} + \mu_{o,\omega,l}^{\delta_{ref}} = 0 \quad n = 1 \quad (28)$$

$$\sum_{n^f} S_l \mu_{o,\omega,l}^f - \sum_{n^t} S_l \mu_{o,\omega,l}^{\bar{f}} - \mu_{o,\omega,l}^{\delta} + \mu_{o,\omega,l}^{\bar{\delta}} = 0 \quad \forall n \neq 1 \quad (29)$$

$$\left. \mu_{\omega,o,n}^{\bar{w}}, \mu_{\omega,o,n}^{\bar{c}}, \mu_{\omega,o,n}^{\bar{g}}, \alpha_{\omega} \geq 0 \right\} \quad \forall o, \omega \quad (30)$$

Equation (22) is the strong duality equality and (23)–(26) are the dual constraints of the constraints of the dual problem. Note that the terms  $\sum_{n=1}^N \mu_{\omega,o,n}^{\bar{w}} \bar{p}_n^{\bar{w}} \cdot W_{\omega,n}$  and  $\sum_{n=1}^N \mu_{\omega,o,n}^{\bar{g}} \bar{p}_n^{\bar{g}}$  in (22) introduce nonlinearity, as  $\mu_{\omega,o,n}^{\bar{w}}, \bar{p}_n^{\bar{w}}, \mu_{\omega,o,n}^{\bar{g}}$ , and  $\bar{p}_n^{\bar{g}}$  are all decision variables. We linearise the problem by substituting (22) by (31) and additionally introducing constraints (32)–(34) [7]. In short, the nonlinear terms are substituted for by an auxiliary piecewise integer approximation which uses the investment options for each asset at each node. The full model specification is given in Appendix A. We computationally solve the problem in Julia’s JuMP.jl, using IBM’s CPLEX as a solver. CPLEX is a solver which, as opposed to heuristic optimisation methods, uses convergent mathematical optimisation techniques so that it arrives at global optima. We moreover check our results for plausibility and find no reason to doubt the verity of our built model.

$$\sum_{n=1}^N c^c p_{\omega,o,n}^c + \sum_{n=1}^N c^g p_{\omega,o,n}^g = \sum_{n=1}^N \lambda_{\omega,o,n} d_{o,n} - \sum_{n=1}^N \mu_{\omega,o,n}^c \bar{p}_{\omega,o,n}^c \quad (31)$$

$$- \sum_{n=1}^N \sum_q z_{nqw}^{aux} \cdot W_{n,\omega} - \sum_{n=1}^N \sum_q z_{nqg}^{aux}$$

$$z_{nqa}^{aux} = \mu_{na}^a - z_{nqa}^{aux} P_{nqa}^{opt} \quad \forall n, a \quad (32)$$

$$0 \leq z_{nqa}^{aux} \leq u_{nqa}^{opt} M \quad \forall n, q \quad (33)$$

$$0 \leq \hat{z}_{nqa}^{aux} \leq (1 - u_{nqa}^{opt}) M \quad \forall n, q \quad (34)$$

### 3. Numerical Experiment

#### 3.1. Assumptions

We test our multi-objective GEP model on a three-node system with a heterogeneous landscape roughly resembling the geographic and demographic profiles of three locations in Wyoming, USA. Our test data reflect the following features. Node one resembles a medium-sized city of about 100,000 inhabitants in a plains region sheltered by mountains. It has a high load demand, relatively low wind speeds and limited capacity to invest in generation facilities due to limited space. Node two represents a suburban small town with an above average industrial base, implying that it has a higher per capita power consumption. It houses about 5000 inhabitants, has relatively high wind speeds, as it is located on a more exposed plain and has plenty of space to install additional generation facilities. Finally, node three is a sparsely populated mountain area. Its load demand is very low, wind speeds are very high and there is plenty of room available to install wind turbines. Due to the mountainous terrain, though, its possibilities to build larger scale power plants are limited. Figure 2 provides a schematic overview over our test system.

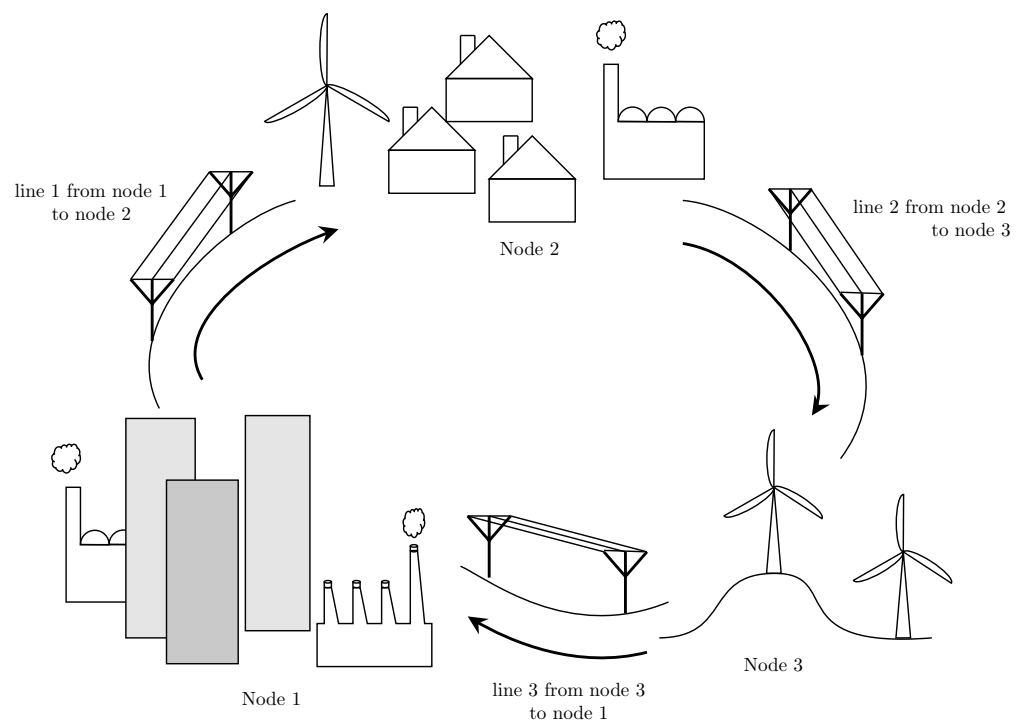


**Figure 2.** Schematic depiction of our test power system.

Due to the mountains separating the three locations, we assume them to be sufficiently geographically isolated for the wind speeds to be independent of one another. The probability density function (PDF) of wind speeds can be expressed as a Rayleigh distribution, as a function of the area's average wind speed [44]. Figure 3a shows the distributions of wind speeds at each node, given the locations' respective average wind speeds. We discretise the PDFs into 10 scenarios with an assigned probability at each node by means of a Monte Carlo Simulation approach. The function to transform wind speeds into electrical power is assumed to be linear between cut-in speed and rated speed and is taken from [45]. The cut-in-, rated- and cut-out speeds are chosen at 8, 31, and 51 MPh, respectively. Using this, we transform each scenario's wind speed into the capacity usage in that scenario to attain parameter  $W_{\omega,n}$ , resulting in the scenarios shown in Figure 3b. This in hand, we construct Kronecker's product of all independent scenarios to acquire our entire set of stochastic scenarios. We moreover assume that the transmission line capacity is equal between all nodes and that there is no transmission loss, i.e., the line susceptance  $S_l$  is equal to the line's transmission capacity  $\bar{f}_l$ .

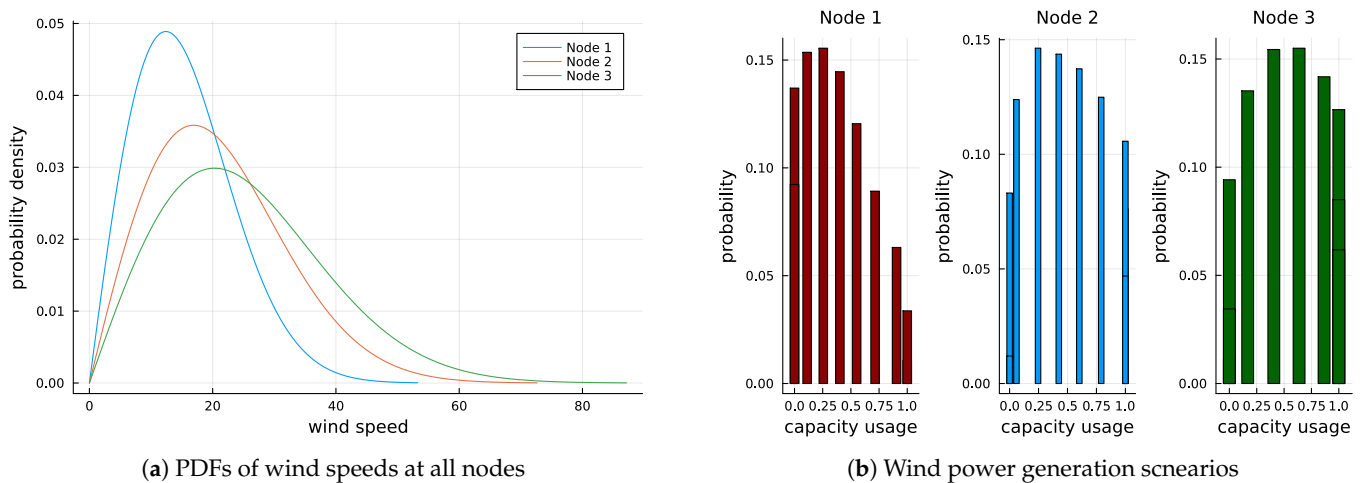


**Figure 3.** The probability density functions of wind speeds in Mph at each node are shown in (a); (b) shows the resulting scenarios, denoting the proportion of rated power  $W_{\omega,p,n}$  and their respective probabilities.

As described above, our experiment resembles locations in Wyoming, USA. Naturally, the data provided by the U.S. Energy Information Administration (EIA) may differ from a European case, inter alia, in resource prices, average wind speeds and usage patterns. Moreover, with the energy crisis ongoing at the time of writing this (fall 2022), stable prices and expectations are hard to come by. We primarily rely on data provided by the EIA and the U.S. Office of Energy Efficiency & Renewable Energy. We calculate variable resource prices as their average between January and July 2022. Following [34], we consider three levels of load demand, each covering a third of the year. These levels  $d_0$  are base load, medium load, and peak load, with factors 1, 1.5, and 2.

We collect data on CO<sub>2</sub>eq GHG emissions per MWhel for both coal and natural gas from [46]. The input efficiency of each generation type is taken from [47]. We use natural gas price data from [48] and coal prices from [49]. For both of them, we use the average of monthly prices between January and June 2022. For coal, we also use the average between the price of Central Appalachian and Powder Basin coal. From the input efficiency and the factor prices, we calculate the generation price per MWhel. We draw on [50] for typical values for cut-in speed, rated speed, and cut-out speed of wind turbines and use [51] for an estimate of the average wind speeds at our nodes. An approximate value for the per capita usage of electricity in Wyoming comes from [52]. We calculate annualised investment costs by drawing on data on overnight- and maintenance cost provided by [53]. The lifespans of wind- and gas turbines come from [40] and [54], respectively. As a simplification, we

assume discount- and inflation rates of zero. Naturally, coal plants also have a fixed annual maintenance cost. Because decommissioning of existing plants is not considered here, though, these costs do not affect the GEP problem and are thus not included. Table 2 shows the node specific parameter values used in the experiment. Table 3 shows the chosen parameter values for each source of power generation. We moreover set the baseline transmission capacity of all lines  $\bar{f}$  to 75 MW and the average value of the lost load  $c^L$  to 250.

**Table 2.** Investment and cost parameters.

	Node 1	Node 2	Node 3
max additional wind cap. in MW	120	540	840
max additional gas cap. in MW	200	400	200
base load in MWh	219	53	11
medium load in MWh	328	79	17
peak load in MWh	437	105	22
average wind speed in Mph	11	15	18

**Table 3.** Parameters specific to each energy carrier.

	Wind	Coal	Natural Gas
annualised investment cost per MW in \$US	10,000	—	28,000
minimum unit increment in capacity expansion	60 MW	—	50 MW
variable cost in $\frac{\$US}{MWh_{el}}$	0	$\approx 29$	$\approx 58$
CO <sub>2</sub> eq emissions in $\frac{tCO_2}{MWh_{el}}$	0	$\approx 1$	$\approx 0.41$

### 3.2. Results

Below, we discuss the findings of the numerical experiment described in Section 3.1. Figure 4a shows the Pareto Frontier with respect to the policymaker's preferences regarding the valuation of the social detriment of GHG emissions for our model specification. Every point on the curve relates to the optimal trade-off between cost and emissions at the given level of SCC. The resulting optimal policy decision and the respective expected total system costs are shown in Figure 4b. The orange line shows the optimal GHG-restriction at each preference level, while the blue line depicts the associated annualised cost of investment, generation and loss of load. The sharp decrease of allowed emissions from a valuation of about \$30 per tCO<sub>2</sub> resembles the fact that it then becomes socially optimal to replace coal power plants with natural gas turbines. The second jump in the optimal policy beyond \$220 can be attributed to the point that partially accepting some loss of load becomes rational. As can clearly be seen from Figure 4, in our specification, it becomes rational to forego almost all fossil fuel based generation from an SCC of \$468 onwards, as generation from gas turbines becomes less attractive than suffering the cost associated with the loss of load. This can also be seen in the massive jump in expected system cost from that point onwards.

We moreover analyse the effect of different SCC preferences on capacity investment and the implied expected generation. Figure 5a shows the cumulative optimal investment decisions in both wind- and gas turbines for each SCC. It can easily be seen that investment in gas infrastructure becomes increasingly important at medium levels of SCC, when replacing coal, while quickly decreasing at higher levels as a result of being itself replaced by both wind turbines with relatively low capacity factors and by loss of load. Figure 5b shows the cumulative expected generation by asset, also including loss of load, with respect to SCC. Unsurprisingly, emission-intensive coal production is dropping very quickly with increasing levels of SCC, being replaced by natural gas. Notably, the expected wind power production is relatively unchanged over the preference space, even though the investment in wind turbines increases quite constantly. This can be explained by the

limitation in transmission capacity. While installing wind turbines in at the mountainous node 3 and even at the moderately windy node 2 is always somewhat attractive, the maximum transmission capacity to the load hungry node 1 is always 75 MW. The increases in wind power capacity with rising SCC are simply replacing coal and gas generation in lower wind speed scenarios. Again, from an SCC of \$468 onwards, one can easily see that the decrease in expected gas power generation is fully compensated by additional loss of load.

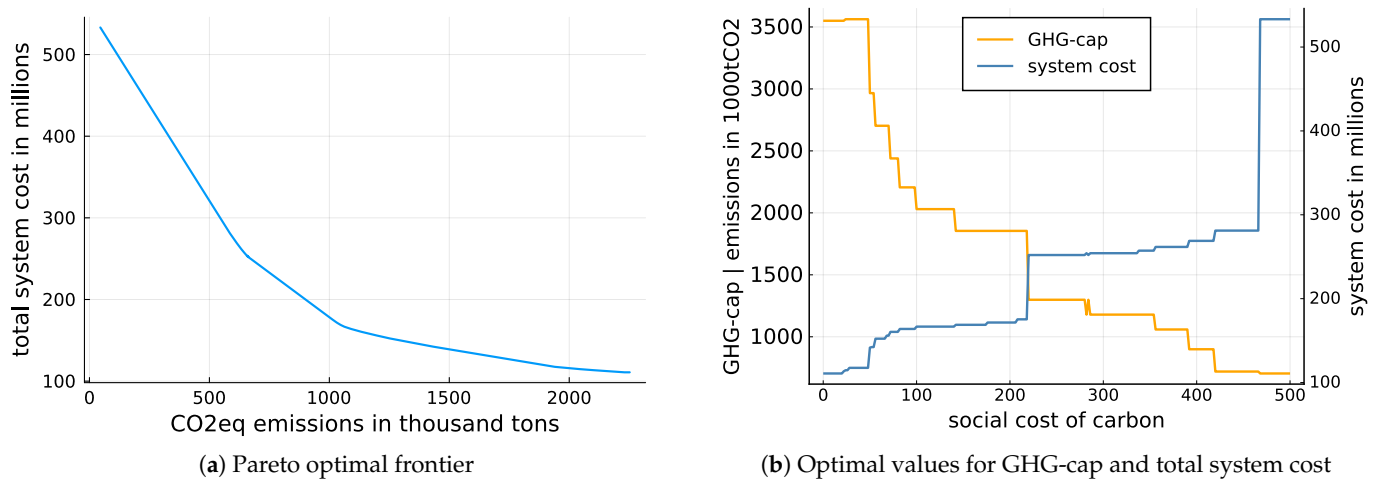


**Figure 4.** (a) shows the Pareto optimal frontier for trading off the total cost of generation against total GHG emissions. Every point on the shown frontier is an optimal solution with respect to the policymaker's a priori preference relation regarding both objectives; (b) shows the resulting policy decision dependent on the chosen level of SCC, as well as the associated expected total system cost in millino \$US.

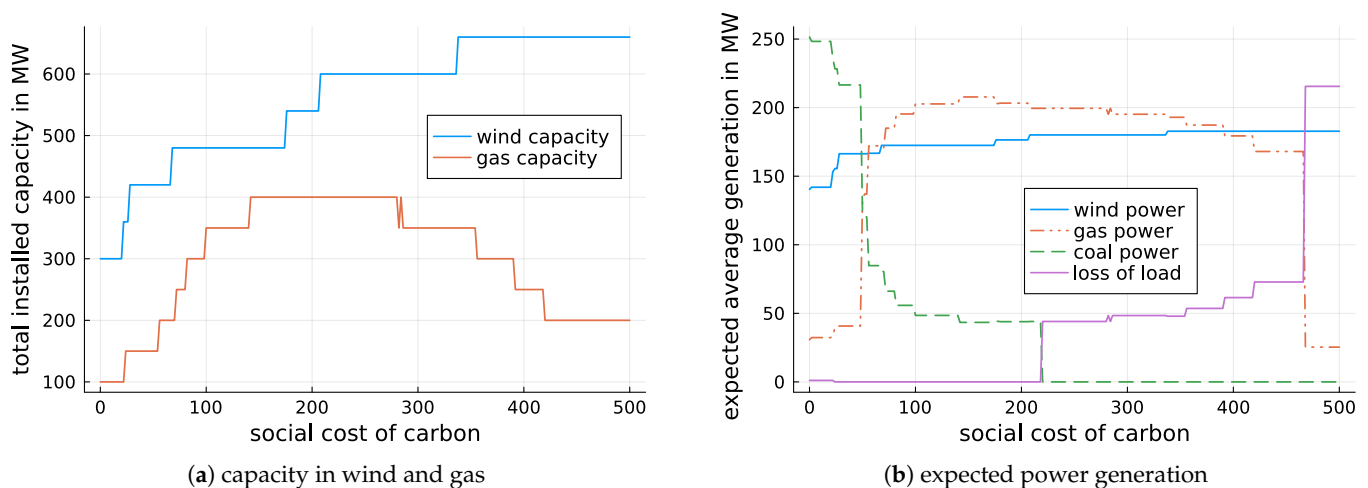


**Figure 5.** The cumulative capacity installments of both wind- and gas turbines with respect to SCC are shown in (a); (b) shows the expected generation of each asset (including loss of load) under each GHG-emissions preference.

Figure 6 shows the nodal power balance for three distinct scenarios under our experimental specification. Figure 6a depicts the corner case in which the societal detriment of GHG emissions is fully disregarded. It can easily be seen that power generation in this scenario relies mostly on cheap coal, while there is still some investment in wind power capacity at nodes 2 and 3. Figure 6b depicts a case in which the cost of carbon is valued at \$50, roughly the magnitude of the mean value found in the review study by [41]. The largest difference to the first case is that the power consumption at node 1 is now mostly



covered using gas power. Moreover, a larger proportion of the load demanded at both nodes 2 and 3 is supplied using wind power. The third case depicted in Figure 6c shows the expected power generation at a higher level of SCC at \$180 per tCO<sub>2</sub> under our specification. This value resembles the call that Fridays for Future Germany put out for an official “fair” emissions price [55], and also roughly equals the 2020 mean estimate of environmentalist think tank Resources for the Future [56].

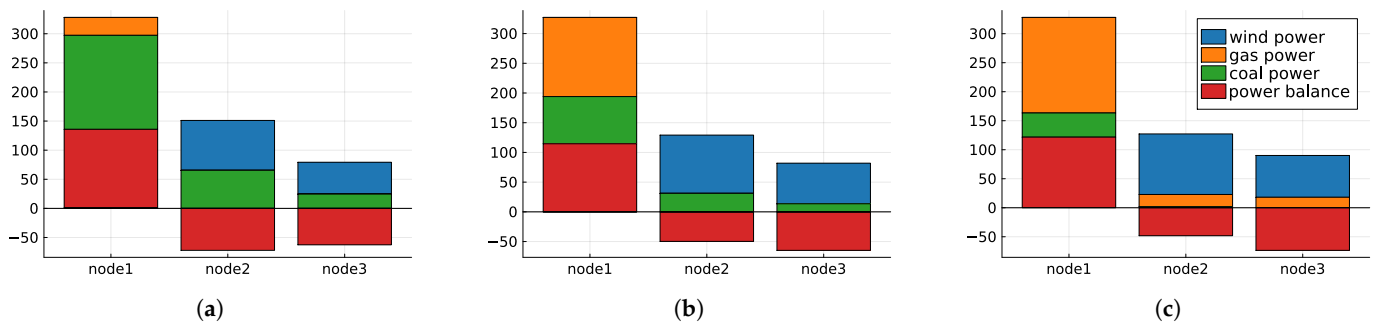


**Figure 6.** The disaggregation of nodal power balances are shown for three relevant scenarios. (a) SCC = 0; (b) SCC = 50; (c) SCC = 180.

There is actually relatively little difference to Figure 6b, predominantly additional replacement of coal by natural gas as well as some additional wind power investment. This holds only as long as the policy area in question is heavily transmission constrained, though. Analysing scenarios with other transmission line capacities, it can be seen that an increase in the overall transmission capacity can decrease both system cost and GHG emissions, but particularly strongly restricting transmission lines can induce considerable losses in social welfare, both in terms of cost and the environment, as can be seen in Figure 7.

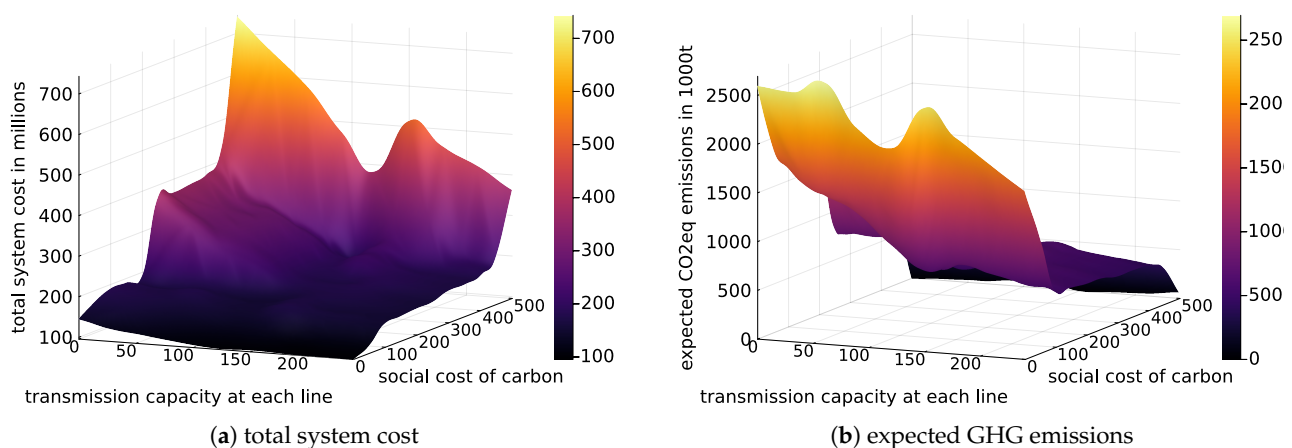


**Figure 7.** (a) shows the total system cost in millions of \$US with respect to both the valuation of GHG emissions and the transmission line capacity; (b) shows the CO<sub>2</sub>eq emissions for the same observation space.

Naturally, the economic valuation of unserved load also greatly affects optimal decision-making. For our benchmark scenario, we assumed a high value of \$250 to retain a relatively high service level for most SCC preferences. As a sensitivity analysis, we test different configurations of the valuation of both loss of load and GHG emissions. The resulting initial system cost and emissions are depicted in Figure 8.

Notably, the resulting optimal decisions are highly dependent on the combination of both valuations, not just their absolute height. This is true for the total system cost in particular. Figure 8a shows that the highest total cost is actually incurred at medium levels of the cost of loss of load, combined with a high SCC. This can be explained by the fact

that, at this configuration, loss of load is so costly that it substantially increases the total incurred cost, while still being sufficiently small in comparison to the social cost of carbon to make a lower service level acceptable. Figure 8b yields relatively foreseeable results. Unsurprisingly, total emissions are highest in any case if SCC is assumed very small. On the other hand, the most mitigation is achieved when the cost of unserved load demand is valued only little in comparison to GHG emissions, as it then becomes more attractive to simply generate less electricity to decrease emissions.

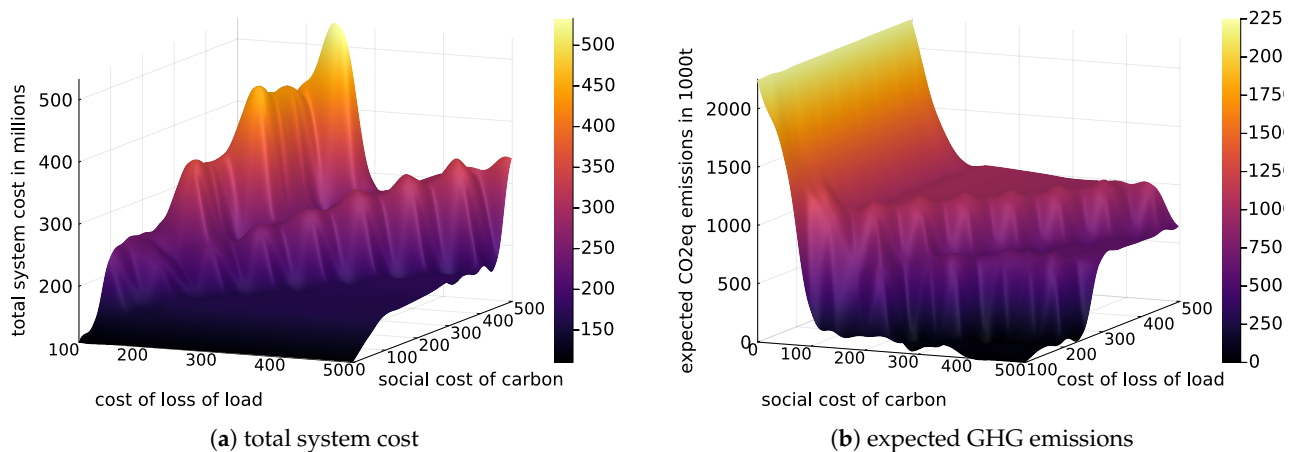


**Figure 8.** (a) shows the total system cost in millions of \$US with respect to both the valuation of GHG emissions and unserved load demand. (b) analogously shows the CO<sub>2</sub>eq emissions. Note that the axes of (a,b) are flipped for better readability.

#### 4. Discussion

We tested our model in a numerical experiment, tuned to relatively realistic conditions. Our results moreover allow for several conclusions: firstly—transmission matters. The worst-case scenarios found were always those with minimum line capacity. Installing a powerful transmission grid can thus enable the rollout of RES, as it allows power flow between the locations best suited for generation and those with the highest load demands.

Our experiment also showed that often either non-negligible parts of the generated wind power were shed or the turbines were not even put up, since the combination of expected local loads and limited transmission lines would have made the investment irrational. Besides an expanded grid, options like decentralised storage or demand side management could help to mitigate that barrier. Relatedly, it might also be advisable to incentivise energy intensive operations to set up closer to the generation centres to allow for a better facility usage.

It was also evident that coal became unattractive at most assumed levels of SCC, even while it was the only technology for which facilities were already in place in our specification. Natural gas, on the other hand, was relatively attractive even at higher levels of SCC, due to its much lower GHG contents. Naturally, gas prices are difficult to foresee with the current crisis at hand. However, it seems plausible that, even at very high prices, natural gas will remain an important factor in the power sector, also due to its beneficial ramping constraints, until quickly dispatchable solutions such as hydrogen peakers, battery storage systems and demand response management will be able to fill the role of gas peakers at scale.

Generally, our results are in line with what theory would suggest, as well as with the dynamics found by other researchers (as far as numerical experiments with different specifications are comparable). Natural gas, for instance, is found to keep playing an important role, even with high penetration of RES, due to its flexibility and lower carbon intensity when compared to, e.g., coal [27,57]. Particularly, more gas is needed if a stricter emissions cap is introduced (up to a certain point) [58]. Unsurprisingly, others also found that *ceteris paribus* increasing the transmission capacity for resources would lower their

on-site factor costs (e.g., [11]). Moreover, putting a higher monetary value on the societal detriment of emissions is also found to increase total system cost as more costly but less emitting generation technologies are used [27,28].

## 5. Conclusions

In this paper, we were seeking to answer the question of how policy-makers could make optimal decisions in trading off between system cost and GHG emissions, with respect to their value judgments. Particularly, we therein accounted for generation stochasticity and optimal operational decisions in a geographically heterogeneous landscape.

We showed how to solve an exemplary version of this problem using three possible generation technologies, including wind power as a stochastic renewable power source. Our model does not cover all generation technologies, but our approach could be extended to incorporate additional elements without thereby introducing particular issues. To arrive at our solution, we developed a multi-objective bilevel stochastic programme to assist policymakers in finding good trade-offs between economic performance and limiting GHG emissions. The application relies on the policymaker's a priori preference relation of emissions and short-term cost.

An extended version of our model tuned to the specifics of a policymakers' region could assist them to plan ahead for the development of their constituency. They could, for instance, use their value judgement to define a search area of SCC values and use the results conjointly determine targets for generation facility expansion and emissions regulation. Based on this plan, they could implement policy measures, such as incentive schemes, to steer the local sector development towards their set targets. This can be primarily useful to smaller constituencies without comprehensive sets of regulation in place, as our method relates to the earlier stages of planning the setup of such a regulatory system. Particularly, this might be interesting for some subnational areas in developing Asia or Africa, as these regions have very high shares of GHG emissions from electricity generation (see Section 1.1).

In our work, we focused on the issue of wind power generation in a heterogeneous landscape. To keep our model tractable and emphasise the core of our considerations, we deliberately left out some circumstances. Thus, our specification still has several limitations that should be overcome in future work in order to make it applicable in the real world. Firstly, we only consider a limited number of exemplary generation technologies. This could be extended through the inclusion of a full set of available technologies, in particular other renewable energy sources like photovoltaics. Moreover, besides RES generation, other stochastic elements govern electricity market outcomes. Other sources of uncertainty like variable load and fluctuations in factor prices should be incorporated as well. Furthermore, the investment plan could be made more realistic and efficient by making explicit other relevant investment options, such as storage and transmission capacity. Finally, we chose a static model for simplicity. A more faithful representation of reality could include a dynamic version of this optimisation problem, including issues such as planning- and construction times.

**Author Contributions:** Conceptualization, L.S., S.T. and W.K.; methodology, L.S. and S.T.; software, L.S.; validation, S.T. and W.K.; formal analysis, L.S. and S.T.; data curation, L.S.; writing—original draft preparation, L.S.; writing—review and editing, S.T. and W.K.; visualization, L.S.; supervision, S.T. and W.K. All authors have read and agreed to the published version of the manuscript.

**Funding:** This research received no external funding.

**Data Availability Statement:** Additional data are available upon request.

**Acknowledgments:** We thank Philipp A. Kienscherf for helping the project start through knowledge and ideas and Simone Horstmann for assisting the project wherever possible.

**Conflicts of Interest:** The authors declare no conflict of interest.

## Nomenclature

Variable	Description	Variable	Description
<b>Indices:</b>			
$o$	Demand level	$\overline{p}_n^w$	Wind power capacity expansion at node $n$
$\omega$	Wind scenario		
$n$	Node	$\overline{p}_n^g$	Gas power capacity expansion at node $n$
$a$	Asset	$u_{nqa}^{opt}$	Investment option (binary) is set to 1 for the optimal investment option
$q$	investment decision	$\overline{G}$	Emissions cap
$l$	Line		
<b>Parameters:</b>			
$SCC$	Social cost of carbon per unit of CO <sub>2</sub> eq emission	$p_{\omega,o,n}^c$	Amount of power supplied by coal
$I_w$	Annualised investment costs per MW of wind capacity installed	$p_{\omega,o,n}^g$	Amount of power supplied by gas
$I_g$	Annualised investment costs per MW of gas capacity installed	$p_{\omega,o,n}^w$	Amount of power supplied by wind
$P_{n,q,a}^{opt}$	Investment of size $q$ in asset class $a$ at nodes $n$	$L_{\omega,o,n}$	Loss of load
$\rho_o$	Hours per year in operating condition $o$	$f_{\omega,o}^f$	Power flow through transmission line coming from node $n$
$\Phi_\omega$	Probability of wind power scenario $\omega$	$f_{\omega,o}^t$	Power flow through transmission line running to node $n$
$c^c$	Unit costs of power supplied by coal	$f_{o,\omega,l}$	Power flow through line $l$
$c^g$	Unit costs of power supplied by gas	$\delta_{o,\omega,l}^f$	Voltage angle at sending node
$c^L$	Cost associated with one unit of lost load	$\delta_{o,\omega,l}^t$	Voltage angle at receiving node
$G^c$	Emissions associated with one unit of electrical energy produced from coal	<b>Dual variables:</b>	
$G^g$	Emissions associated with one unit of electrical energy produced from gas	$\lambda_{\omega,o}$	Marginal nodal price of generation
$\overline{f}_l$	Flow capacity of line $l$	$\mu_{\omega,o}^w$	Shadow price of wind power capacity
$S_l$	Susceptance of line $l$	$\mu_{\omega,o}^g$	Shadow price of gas power capacity
$W_{\omega,n}$	wind conditions at in scenario $\omega$ at node $n$	$\mu_{\omega,o}^c$	Shadow price of coal power capacity
$d_{o,n}$	load demand at node $n$ & demand level $o$	$\alpha_w$	Dual variable of the emissions constraint
<b>Dual variables of transmission constraints:</b>			
$\mu_{o,\omega,l}^{\overline{f}}, \mu_{o,\omega,l}^{\underline{f}}, \mu_{o,\omega,l}^f, \mu_{o,\omega,l}^{\overline{\delta}}, \mu_{o,\omega,l}^{\underline{\delta}}, \mu_{o,\omega,l}^{\delta_{ref}}$			
<b>Auxiliary variables:</b>			
$z_{nqa}^{aux}, z_{nqa}^{ux}$			

## Appendix A. Full Model Specification

$$\min_{\Delta_{SL}} \sum_{n=1}^N (I_w^w \overline{p}_n^w + I_g^g \overline{p}_n^g) + \sum_{o=1}^O \rho_o \sum_{\omega=1}^{\Omega} \Phi_\omega \sum_{n=1}^N (c^c p_{\omega,o,n}^c + c^g p_{\omega,o,n}^g + \sum_{n=1}^N c^L L_{\omega,o,n}) \quad (A1)$$

$$+ SCC \cdot \sum_{\omega=1}^{\Omega} \Phi_\omega \sum_{o=1}^O \rho_o \sum_{n=1}^N (p_{\omega,o,n}^c G^c + p_{\omega,o,n}^g G^g)$$

$$s.t. \left\{ \begin{array}{l} \overline{p}_n^w = \sum_q u_{nqa=w}^{opt} P_{nqa=w}^{opt} \end{array} \right. \quad (A2)$$

$$\overline{p}_n^g = \sum_q u_{nqa=g}^{opt} P_{nqa=g}^{opt} \quad (A3)$$

$$\sum_q u_{nqa=w}^{opt} = 1 \quad (A4)$$

$$\sum_q u_{nqa=g}^{opt} = 1 \quad (A5)$$

$$u_{nqa=w}^{opt}, u_{nqa=g}^{opt} \in \{0, 1\} \forall q \} \forall n, a \quad (A6)$$

$$\overline{G} \geq 0 \quad (A7)$$

$$\sum_{n=1}^N c^c p_{\omega,o,n}^c + \sum_{n=1}^N c^g p_{\omega,o,n}^g + \sum_{n=1}^N c^L L_{\omega,o,n} = \sum_{n=1}^N \lambda_{\omega,o,n} d_{o,n} - \sum_{n=1}^N \mu_{\omega,o,n}^{\bar{c}} \bar{p}_{\omega,o,n}^c \quad (\text{A8})$$

$$- \sum_{n=1}^N \sum_q z_{nqa}^{aux} \cdot W_{n,\omega} - \sum_{n=1}^N \sum_q z_{nqa}^{aux} \quad (\text{A9})$$

$$z_{nqa}^{aux} = \mu_{na}^{\bar{a}} - z_{nqa}^{aux} p_{nqa}^{opt} \quad \forall n, a \quad (\text{A9})$$

$$0 \leq z_{nqa}^{aux} \leq u_{nqa}^{opt} M \quad \forall n, q \quad (\text{A10})$$

$$0 \leq z_{nqa}^{aux} \leq (1 - u_{nqa}^{opt}) M \quad \forall n, q \quad (\text{A11})$$

$$\left\{ \begin{array}{l} p_{\omega,o,n}^w + p_{\omega,o,n}^c + p_{\omega,o,n}^g - f_{\omega,o,n}^f + f_{\omega,o,n}^t = d_{o,n} \\ 0 \leq p_{\omega,o,n}^w \leq \bar{p}_n^w \cdot W_{\omega,n} : \mu_{\omega,o,n}^{\bar{w}} \\ 0 \leq p_{\omega,o,n}^c \leq \bar{p}_n^c : \mu_{\omega,o,n}^{\bar{c}} \\ 0 \leq p_{\omega,o,n}^g \leq \bar{p}_n^g : \mu_{\omega,o,n}^{\bar{g}} \end{array} \right\} \quad \forall \omega, o, n \quad (\text{A12})$$

$$0 \leq p_{\omega,o,n}^w \leq \bar{p}_n^w \cdot W_{\omega,n} : \mu_{\omega,o,n}^{\bar{w}} \quad (\text{A13})$$

$$0 \leq p_{\omega,o,n}^c \leq \bar{p}_n^c : \mu_{\omega,o,n}^{\bar{c}} \quad (\text{A14})$$

$$0 \leq p_{\omega,o,n}^g \leq \bar{p}_n^g : \mu_{\omega,o,n}^{\bar{g}} \quad (\text{A15})$$

$$\sum_{n=1}^N \sum_{o=1}^O \rho_o \cdot [p_{\omega,o,n}^c G^c + p_{\omega,o,n}^g G^g] \leq \bar{G} : \alpha_{\omega} \quad \forall \omega \quad (\text{A16})$$

$$\left\{ \begin{array}{l} -\bar{f}_l \leq f_{o,\omega,l} \leq \bar{f}_l : \mu_{o,\omega,l}^{\bar{f}}, \mu_{o,\omega,l}^f \quad \forall l \\ f_{o,\omega,l} = S_l (\delta_{o,\omega,l}^f - \delta_{o,\omega,l}^t) : \mu_{o,\omega,l}^f \quad \forall l \\ -\pi \leq \delta_{o,\omega,l} \leq \pi : \mu_{o,\omega,l}^{\bar{\delta}}, \mu_{o,\omega,l}^{\delta} \quad \forall n \\ \delta_{o,\omega,1} = 0 : \mu_{o,\omega,1}^{\delta_{ref}} \end{array} \right\} \quad \forall o, \omega \quad (\text{A17})$$

$$f_{o,\omega,l} = S_l (\delta_{o,\omega,l}^f - \delta_{o,\omega,l}^t) : \mu_{o,\omega,l}^f \quad \forall l \quad (\text{A18})$$

$$-\pi \leq \delta_{o,\omega,l} \leq \pi : \mu_{o,\omega,l}^{\bar{\delta}}, \mu_{o,\omega,l}^{\delta} \quad \forall n \quad (\text{A19})$$

$$\delta_{o,\omega,1} = 0 : \mu_{o,\omega,1}^{\delta_{ref}} \quad (\text{A20})$$

$$\left\{ \begin{array}{l} -\lambda_{\omega,o,n} + \mu_{\omega,o,n}^{\bar{w}} \geq 0 \quad \forall n \\ c^c - \lambda_{\omega,o,n} + \alpha_{\omega,o,n} \cdot \rho_o \cdot G^c + \mu_{\omega,o,n}^{\bar{c}} \geq 0 \quad \forall n \\ c^g - \lambda_{\omega,o,n} + \alpha_{\omega,o,n} \cdot \rho_o \cdot G^g + \mu_{\omega,o,n}^{\bar{g}} \geq 0 \quad \forall n \\ c^L - \lambda_{\omega,o,n} \geq 0 \quad \forall n \end{array} \right\} \quad (\text{A21})$$

$$c^c - \lambda_{\omega,o,n} + \alpha_{\omega,o,n} \cdot \rho_o \cdot G^c + \mu_{\omega,o,n}^{\bar{c}} \geq 0 \quad \forall n \quad (\text{A22})$$

$$c^g - \lambda_{\omega,o,n} + \alpha_{\omega,o,n} \cdot \rho_o \cdot G^g + \mu_{\omega,o,n}^{\bar{g}} \geq 0 \quad \forall n \quad (\text{A23})$$

$$c^L - \lambda_{\omega,o,n} \geq 0 \quad \forall n \quad (\text{A24})$$

$$\lambda_{o,\omega,l}^f - \lambda_{o,\omega,l}^t - \mu_{o,\omega,l}^f - \mu_{o,\omega,l}^{\bar{f}} - \mu_{o,\omega,l}^f = 0 \quad \forall l \quad (\text{A25})$$

$$\sum_{n^f} S_l \mu_{o,\omega,l}^f - \sum_{n^t} S_l \mu_{o,\omega,l}^f + \mu_{o,\omega,l}^{\delta_{ref}} = 0 \quad n = 1 \quad (\text{A26})$$

$$\sum_{n^f} S_l \mu_{o,\omega,l}^f - \sum_{n^t} S_l \mu_{o,\omega,l}^f - \mu_{o,\omega,l}^{\delta} + \mu_{o,\omega,l}^{\bar{\delta}} = 0 \quad \forall n \neq 1 \quad (\text{A27})$$

$$\left\{ \begin{array}{l} \mu_{\omega,o,n}^{\bar{w}}, \mu_{\omega,o,n}^{\bar{c}}, \mu_{\omega,o,n}^{\bar{g}}, \alpha_{\omega} \geq 0 \end{array} \right\} \quad \forall o, \omega \quad (\text{A28})$$

## References

1. IEA. IEA CO<sub>2</sub> Emissions from Fuel Combustion Statistics: Greenhouse Gas Emissions from Energy. Available online: [https://www.oecd-ilibrary.org/energy/data/iea-co2-emissions-from-fuel-combustion-statistics\\_co2-data-en](https://www.oecd-ilibrary.org/energy/data/iea-co2-emissions-from-fuel-combustion-statistics_co2-data-en) (accessed on 21 September 2022).
2. IPCC. *Climate Change 2022: Mitigation of Climate Change. Contribution of Working Group III to the Sixth Assessment Report of the Intergovernmental Panel on Climate Change*; Technical Report; IPCC: Cambridge, UK; New York, NY, USA, 2022.
3. IEA. *World Energy Outlook 2021*; IEA: Paris, France, 2021.

4. Ekardt, F. *Sustainability: Transformation, Governance, Ethics, Law*, 3rd ed.; Environmental Humanities: Transformation, Governance, Ethics, Law; Springer International Publishing: Cham, Switzerland, 2020. [\[CrossRef\]](#)
5. Stern, D.I. Energy and economic growth. In *Routledge Handbook of Energy Economics*, 1st ed.; Soytaş, U., Sarı, R., Eds.; Routledge: Milton Park, UK, 2019. [\[CrossRef\]](#)
6. Khezri, R.; Mahmoudi, A. Review on the state-of-the-art multi-objective optimisation of hybrid standalone/grid-connected energy systems. *IET Gener. Transm. Distrib.* **2020**, *14*, 4285–4300. [\[CrossRef\]](#)
7. Conejo, A.J.; Baringo Morales, L.; Kazempour, S.J.; Siddiqui, A.S. *Investment in Electricity Generation and Transmission*; Springer International Publishing: Cham, Switzerland, 2016. [\[CrossRef\]](#)
8. Ning, Y.; Chen, K.; Zhang, B.; Ding, T.; Guo, F.; Zhang, M. Energy conservation and emission reduction path selection in China: A simulation based on Bi-Level multi-objective optimization model. *Energy Policy* **2020**, *137*, 111116. [\[CrossRef\]](#)
9. Zhou, S.; Yang, J.; Yu, S. A Stochastic Multi-Objective Model for China's Provincial Generation-Mix Planning: Considering Variable Renewable and Transmission Capacity. *Energies* **2022**, *15*, 2797. [\[CrossRef\]](#)
10. Chen, F.; Huang, G.; Fan, Y. A linearization and parameterization approach to tri-objective linear programming problems for power generation expansion planning. *Energy* **2015**, *87*, 240–250. [\[CrossRef\]](#)
11. Valle, A.d.; Wogrin, S.; Reneses, J. Multi-objective bi-level optimization model for the investment in gas infrastructures. *Energy Strategy Rev.* **2020**, *30*, 100492. [\[CrossRef\]](#)
12. Aldarajee, A.H.M.; Hosseinian, S.H.; Vahidi, B.; Dehghan, S. Security constrained multi-objective bi-directional integrated electricity and natural gas co-expansion planning considering multiple uncertainties of wind energy and system demand. *IET Renew. Power Gener.* **2020**, *14*, 1395–1404. [\[CrossRef\]](#)
13. Aghaei, J.; Akbari, M.A.; Roosta, A.; Baharvandi, A. Multiobjective generation expansion planning considering power system adequacy. *Electr. Power Syst. Res.* **2013**, *102*, 8–19. [\[CrossRef\]](#)
14. Gong, J.W.; Li, Y.P.; Lv, J.; Huang, G.H.; Suo, C.; Gao, P.P. Development of an integrated bi-level model for China's multi-regional energy system planning under uncertainty. *Appl. Energy* **2022**, *308*, 118299. [\[CrossRef\]](#)
15. Yang, Y.; Luo, Z.; Yuan, X.; Lv, X.; Liu, H.; Zhen, Y.; Yang, J.; Wang, J. Bi-Level Multi-Objective Optimal Design of Integrated Energy System Under Low-Carbon Background. *IEEE Access* **2021**, *9*, 53401–53407. [\[CrossRef\]](#)
16. Marler, R.T.; Arora, J.S. The weighted sum method for multi-objective optimization: New insights. *Struct. Multidiscip. Optim.* **2010**, *41*, 853–862. [\[CrossRef\]](#)
17. Oree, V.; Sayed Hassen, S.Z.; Fleming, P.J. Generation expansion planning optimisation with renewable energy integration: A review. *Renew. Sustain. Energy Rev.* **2017**, *69*, 790–803. [\[CrossRef\]](#)
18. Asgharian, V.; Abdelaziz, M.M.A.; Kamwa, I. Multi-stage bi-level linear model for low carbon expansion planning of multi-area power systems. *IET Gener. Transm. Distrib.* **2019**, *13*, 9–20. [\[CrossRef\]](#)
19. Asgharian, V.; Genc, V.M.I. Multi-objective optimization for voltage regulation in distribution systems with distributed generators. In Proceedings of the 2016 IEEE Electrical Power and Energy Conference (EPEC), Ottawa, ON, Canada, 12–14 October 2016; IEEE: New York, NY, USA, 2016; pp. 1–6. [\[CrossRef\]](#)
20. Hussain, A.; Kim, H.M. Goal-Programming-Based Multi-Objective Optimization in Off-Grid Microgrids. *Sustainability* **2020**, *12*, 8119. [\[CrossRef\]](#)
21. Gorenstin, B.; Campodonico, N.; Costa, J.; Pereira, M. Power system expansion planning under uncertainty. *IEEE Trans. Power Syst.* **1993**, *8*, 129–136. [\[CrossRef\]](#)
22. Hu, Y. An NSGA-II based multi-objective optimization for combined gas and electricity network expansion planning. *Appl. Energy* **2016**, *167*, 280–293. [\[CrossRef\]](#)
23. Park, H.; Baldick, R. Stochastic Generation Capacity Expansion Planning Reducing Greenhouse Gas Emissions. *IEEE Trans. Power Syst.* **2015**, *30*, 1026–1034. [\[CrossRef\]](#)
24. Home-Ortiz, J.M.; Melgar-Dominguez, O.D.; Pourakbari-Kasmaei, M.; Mantovani, J.R.S. A stochastic mixed-integer convex programming model for long-term distribution system expansion planning considering greenhouse gas emission mitigation. *Int. J. Electr. Power Energy Syst.* **2019**, *108*, 86–95. [\[CrossRef\]](#)
25. Conejo, A.J.; Nogales, F.; Arroyo, J. Price-taker bidding strategy under price uncertainty. *IEEE Trans. Power Syst.* **2002**, *17*, 1081–1088. [\[CrossRef\]](#)
26. Mitridati, L.; Pinson, P. A Bayesian Inference Approach to Unveil Supply Curves in Electricity Markets. *IEEE Trans. Power Syst.* **2018**, *33*, 2610–2620. [\[CrossRef\]](#)
27. Fitiwi, D.Z.; Lynch, M.; Bertsch, V. Enhanced network effects and stochastic modelling in generation expansion planning: Insights from an insular power system. *Socio-Econ. Plan. Sci.* **2020**, *71*, 100859. [\[CrossRef\]](#)
28. Zolfaghari Moghaddam, S. Generation and transmission expansion planning with high penetration of wind farms considering spatial distribution of wind speed. *Int. J. Electr. Power Energy Syst.* **2019**, *106*, 232–241. [\[CrossRef\]](#)
29. Hemmati, R.; Hooshmand, R.A.; Khodabakhshian, A. Coordinated generation and transmission expansion planning in deregulated electricity market considering wind farms. *Renew. Energy* **2016**, *85*, 620–630. [\[CrossRef\]](#)
30. Colson, B.; Marcotte, P.; Savard, G. An overview of bilevel optimization. *Ann. Oper. Res.* **2007**, *153*, 235–256. [\[CrossRef\]](#)
31. Kazempour, S.J.; Conejo, A.J. Strategic Generation Investment Under Uncertainty Via Benders Decomposition. *IEEE Trans. Power Syst.* **2012**, *27*, 424–432. [\[CrossRef\]](#)



32. Garces, L.; Conejo, A.J.; Garcia-Bertrand, R.; Romero, R. A Bilevel Approach to Transmission Expansion Planning Within a Market Environment. *IEEE Trans. Power Syst.* **2009**, *24*, 1513–1522. [\[CrossRef\]](#)
33. Li, R.; Wang, W.; Chen, Z.; Wu, X. Optimal planning of energy storage system in active distribution system based on fuzzy multi-objective bi-level optimization. *J. Mod. Power Syst. Clean Energy* **2018**, *6*, 342–355. [\[CrossRef\]](#)
34. Ghaderi, A.; Parsa Moghaddam, M.; Sheikh-El-Eslami, M. Energy efficiency resource modeling in generation expansion planning. *Energy* **2014**, *68*, 529–537. [\[CrossRef\]](#)
35. Acemoglu, D.; Aghion, P.; Bursztyn, L.; Hemous, D. The Environment and Directed Technical Change. *Am. Econ. Rev.* **2012**, *102*, 131–166. [\[CrossRef\]](#)
36. Acemoglu, D.; Akcigit, U.; Hanley, D.; Kerr, W. Transition to Clean Technology. *J. Political Econ.* **2016**, *124*, 52–104. [\[CrossRef\]](#)
37. Rockström, J.; Gaffney, O.; Rogelj, J.; Meinshausen, M.; Nakicenovic, N.; Schellnhuber, H.J. A roadmap for rapid decarbonization. *Science* **2017**, *355*, 1269–1271. [\[CrossRef\]](#)
38. Geels, F.W.; Sovacool, B.K.; Schwanen, T.; Sorrell, S. Sociotechnical transitions for deep decarbonization. *Science* **2017**, *357*, 1242–1244. [\[CrossRef\]](#) [\[PubMed\]](#)
39. Qazi, A.; Hussain, F.; Rahim, N.A.; Hardaker, G.; Alghazzawi, D.; Shaban, K.; Haruna, K. Towards Sustainable Energy: A Systematic Review of Renewable Energy Sources, Technologies, and Public Opinions. *IEEE Access* **2019**, *7*, 63837–63851. [\[CrossRef\]](#)
40. Stehly, T.; Beiter, P.; Duffy, P. *2019 Cost of Wind Energy Review*; Technical Report; National Renewable Energy Laboratory: Golden, CO, USA, 2020.
41. Wang, P.; Deng, X.; Zhou, H.; Yu, S. Estimates of the social cost of carbon: A review based on meta-analysis. *J. Clean. Prod.* **2019**, *209*, 1494–1507. [\[CrossRef\]](#)
42. Carrion, M.; Arroyo, J.; Conejo, A. A Bilevel Stochastic Programming Approach for Retailer Futures Market Trading. *IEEE Trans. Power Syst.* **2009**, *24*, 1446–1456. [\[CrossRef\]](#)
43. Talari, S.; Shafie-khah, M.; Wang, F.; Aghaei, J.; Catalao, J.P.S. Optimal Scheduling of Demand Response in Pre-Emptive Markets Based on Stochastic Bilevel Programming Method. *IEEE Trans. Ind. Electron.* **2017**, *66*, 1453–1464. [\[CrossRef\]](#)
44. Li, Y.; Zio, E. Uncertainty analysis of the adequacy assessment model of a distributed generation system. *Renew. Energy* **2012**, *41*, 235–244. [\[CrossRef\]](#)
45. Talari, S.; Yazdanejad, M.; Haghifam, M. Stochastic-based scheduling of the microgrid operation including wind turbines, photovoltaic cells, energy storages and responsive loads. *IET Gener. Transm. Distrib.* **2015**, *9*, 1498–1509. [\[CrossRef\]](#)
46. EIA. Frequently Asked Questions (FAQs)—U.S. Energy Information Administration (EIA). Available online: <https://www.eia.gov/tools/faqs/faq.php> (accessed on 29 September 2022).
47. EIA. Average Operating Heat Rate for Selected Energy Sources. Available online: [https://www.eia.gov/electricity/annual/html/epa\\_08\\_01.html](https://www.eia.gov/electricity/annual/html/epa_08_01.html) (accessed on 29 September 2022).
48. EIA. U.S. Natural Gas Prices. Available online: [https://www.eia.gov/dnav/ng/ng\\_pri\\_sum\\_dcu\\_nus\\_m.htm](https://www.eia.gov/dnav/ng/ng_pri_sum_dcu_nus_m.htm) (accessed on 29 September 2022).
49. EIA. Electricity Monthly Update—U.S. Energy Information Administration (EIA). Available online: <https://www.eia.gov/electricity/monthly/update/print-version.php> (accessed on 29 September 2022).
50. Office of Energy Efficiency & Renewable Energy. How Do Wind Turbines Survive Severe Storms? Available online: <https://www.energy.gov/eere/articles/how-do-wind-turbines-survive-severe-storms> (accessed on 29 September 2022).
51. Office of Energy Efficiency & Renewable Energy. Wind Turbines: The Bigger, the Better. Available online: <https://www.energy.gov/eere/articles/wind-turbines-bigger-better> (accessed on 29 September 2022).
52. Project, S.E.E. Wyoming Energy Fact Sheet. Available online: <https://www.swenergy.org/Data/Sites/1/media/documents/publications/factsheets/WY-Factsheet.pdf> (accessed on 29 September 2022).
53. EIA. Cost and Performance Characteristics of New Generating Technologies, Annual Energy Outlook 2022. Available online: [https://www.eia.gov/outlooks/aeo/assumptions/pdf/table\\_8.2.pdf](https://www.eia.gov/outlooks/aeo/assumptions/pdf/table_8.2.pdf) (accessed on 4 September 2022).
54. Spath, P.L.; Mann, M.K. *Life Cycle Assessment of a Natural Gas Combined Cycle Power Generation System*; Technical Report; NREL: Cole Boulevard, CO, USA, 2000. [\[CrossRef\]](#)
55. Fridays for Future. Unsere Forderungen an Die Politik | Fridays for Future. Available online: <https://fridaysforfuture.de/forderungen/> (accessed on 30 September 2022).
56. Resources for the Future. Social Cost of Carbon Explorer. Available online: <https://www.rff.org/publications/data-tools/scc-explorer/> (accessed on 30 September 2022).
57. Nguyen, H.T.; Felder, F.A. Generation expansion planning with renewable energy credit markets: A bilevel programming approach. *Appl. Energy* **2020**, *276*, 115472. [\[CrossRef\]](#)
58. Cheng, Y.; Zhang, N.; Kang, C. Bi-Level Expansion Planning of Multiple Energy Systems under Carbon Emission Constraints. In Proceedings of the 2018 IEEE Power & Energy Society General Meeting (PESGM), Portland, OR, USA, 5–10 August 2018; IEEE: New York, NY, USA, 2018; pp. 1–5. [\[CrossRef\]](#)